HOSTED BY
ELSEVIER
CrossMark
Available online at www.sciencedirect.com
ScienceDirect
Defence Technology 12 (2016) 129–133
www.elsevier.com/locate/dt

Study of detonation wave contours in EFP warhead

Xu-dong ZU *, Zheng-xiang HUANG, Chuan-sheng ZHU, Qiang-qiang XIAO

School of Mechanical Engineering, Nanjing University of Science and Technology, Xiaolingwei 200, Nanjing 210094, China

Received 24 July 2015; revised 5 January 2016; accepted 6 January 2016

Available online 25 January 2016

Abstract

An analytical model for calculating the propagation time of shock wave in a wave shaper is presented in this study. The calculated results show that the contours of three typical detonation waves, such as conical detonation wave, spherical detonation wave, and planar detonation wave, can be formed in the main charge by changing the thickness of wave shaper.

The results show that the planar detonation wave do better than the conical detonation and the spherical detonation wave in increasing the length–diameter ratio of explosively-formed projectiles (EFP) and keep the nose of EFP integrated. The detonation wave can increase the length–diameter ratio of EFP when the wave shaper has the suitable thickness.

Keywords: Explosion mechanism; Explosively-formed projectile; Wave shaper; Detonation wave contour

1. Introduction

Explosively-formed projectiles (EFPs) are used in numerous modern ammunition systems because of their advantages of effective stand-off and strong secondary effects after penetration. For the purpose of improving the penetration performance of warheads, one of the design goals of any designer is to obtain the most elongated and compact projectile with a high initial velocity [1]. Powerful explosives [2], detonation wave shaping [3], and the use of high-density and high-ductility liner materials are the main ways to achieve this goal [4]. The detonation wave shaping is considered to be the most efficient way of improving the penetration performance of warheads [5]. Embedding a wave shaper in charge is one of the ways to shape a detonation wave [6–8]. Weimann [1], Murphy et al. [6], and Men et al. [9] reported that the EFP length could be increased if a wave shaper is placed in charge. Zhang et al. [8,10] compared the performances of EFPs formed from warheads with and without wave shaper, and the results indicated that EFP formed from the warhead with a wave shaper has a higher velocity, larger length–diameter ratio, and higher penetration capability compared to that formed without a wave shaper. However, the researchers have not explored how to adjust the detonation wave contours shaped by the thickness of wave shaper on the formation of EFP.

An analytical model for calculating the propagation time of shock wave in the wave shaper is presented in this study. The time of the penetrating detonation wave reaching the liner and the time of the diffracted detonation wave reaching the liner can be determined. The calculated results show that the contours of three typical detonation waves can be formed in the main charge by changing the thickness of wave shaper. The effects of detonation wave contours on the formation of EFP were studied using the LS-DYNA software.

2. Analytical models

2.1. The initial parameters of shock wave in wave shaper

Given that the shock impedance of the Plexiglas is less than that of the explosive, the transmitted wave in wave shaper is a shock wave when the detonation wave impacts the wave shaper which is made of Plexiglas, whereas the reflected wave is a rarefaction wave. The initial parameters of the shock wave in wave shaper can be calculated by the following equation [11]

$$\begin{cases} u_x = \dfrac{D}{\gamma+1}\left\{1+\dfrac{2\gamma}{\gamma-1}\left[1-\left(\dfrac{p_x}{p_{CJ}}\right)^{\frac{\gamma-1}{2\gamma}}\right]\right\} \\ p_x = \rho_{m0}(a+bu_x)u_x \end{cases} \tag{1}$$

Peer review under responsibility of China Ordnance Society.

* Corresponding author. Tel.: +8602584315649.
E-mail address: zuxudong9902@mail.njust.edu.cn (X.D. ZU).

http://dx.doi.org/10.1016/j.dt.2016.01.002

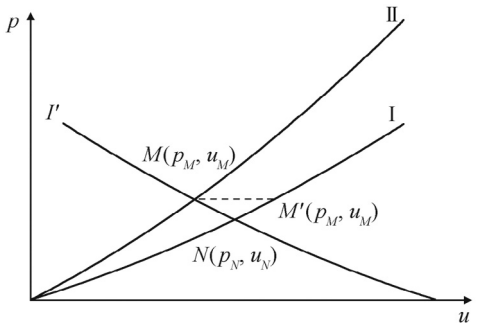

Fig. 1. u–p curves of Plexiglas and main charge.

where D is the velocity of detonation wave; P_{CJ} is the CJ detonation pressure; γ is the exponent in the polytropic equation of state for explosive; u_x is the particle velocity; p_x is the pressure of shock wave; ρ_{m_0} is the density of Plexiglas; and a and b are the material constants of Plexiglas.

2.2. Output parameters of shock wave in wave shaper

Given that the shock impedance of Plexiglas is less than that of the explosive, both the transmitted and reflection waves are the shock waves. The Hugoniot equations of Plexiglas and explosive are

$$p_1 = \rho_{01}(a_1 + b_1 u_x)u_x \tag{2}$$

$$p_2 = \rho_{02}(a_2 + b_2 u_x)u_x \tag{3}$$

As shown in Fig. 1, I and II represent the Hugoniot curves of Plexiglas and explosive, respectively, I' is the mirror curve of I about N, the pressure p_M and particle velocity u_M at the intersection point M are the initial parameters of shock wave in the main charge, M' is the mirror point of M about N, and the pressure p_N and particle velocity u_N at point N are the output parameters of shock wave in the wave shaper.

The criterion of shock wave initiating the explosive adopts the critical pressure criterion. If the critical pressure of the explosive p_c is known, $u_{M'}$ and u_M can be calculated by substituting $p_M = p_c$ into Eqs. (2) and (3). Given that M' is the mirror point of M about N, $u_N = (u_M + u_{M'})/2.0$. Finally, p_N can be calculated by substituting u_N into Eq. (2).

2.3. Critical thickness of wave shaper

Given that the attenuation of shock wave in inert medium is very complex, the attenuation law of shock wave in an inert medium can be expressed as an empirical formula [11]

$$p_x = p_0 e^{-\alpha x} \tag{4}$$

where p_0 is the initial pressure in the inert medium; α is the attenuation coefficient of the inert medium; x is the propagation distance of shock wave in the inert medium; and p_x is the pressure of shock wave corresponding to distance x.

The critical thickness of wave shaper h_c can be determined by substituting the initial pressure p_0 and output pressure p_N in Eq. (4).

2.4. Propagation time of shock wave in wave shaper

The velocity of shock wave in the wave shaper can be expressed as

$$u_s = a + b u_x \tag{5}$$

where u_s is the velocity of shock wave; and a and b are the constants of wave shaper material.

According to Eqs. (2), (4), and (5), the propagation distance x can be expressed as

$$x = -\frac{1}{\alpha}\ln\frac{\rho_{m0}u_s(u_s - a)}{bp_0} \tag{6}$$

A series of points (u_s, x) in the warhead can be obtained from Eq. (6), and the function of u_s about x can be obtained by fitting these points

$$u_s = A\left[(x - B)^2 + C^2\right] \tag{7}$$

The propagation time of shock wave in wave shaper can be written as

$$t = \int_0^h \frac{\mathrm{d}x}{A\left[(x-B)^2 + C^2\right]} = \frac{1}{AB}\left(\arctan\frac{h-B}{C} - \arctan\frac{-B}{C}\right) \tag{8}$$

where h is the thickness of wave shaper; and A, B, and C are constants.

In the calculation, the 8701 explosive which consists of 95% RDX and 5% TNT was used as the subsidiary charge, with $\rho = 1.713$ g/cm^3, $D = 7.98$ mm/μs, and $P_{CJ} = 28.6$ GPa [12]. The material of wave shaper was Plexiglas with $\rho = 1.184$ g/cm^3, $a = 2.572$ mm/μs, and $b = 1.536$ [13]. The material of the main charge was an 8701 explosive with $\rho = 1.7$ g/cm^3, $a = 2.95$ mm/μs, and $b = 1.58$ [14]. The attenuation coefficient, α, of Plexiglas is 0.1186 [15]. The critical pressure of the 8701 explosive is 2.4 GPa [16].

Initial pressure p_0 and particle velocity u_0 in the wave shaper, output pressure p_n, particle velocity u_n, critical thickness h_c of wave shaper, and the constants in Eq. (8) can be determined according to the parameters mentioned above, which are $p_0 = 21.73$ GPa, $u_0 = 2.7194$ mm/μs, $p_N = 1.9288$ GPa, $u_N = 0.49$ mm/μs, $h_c = 20.4$ mm, $A = 0.0053$, $B = 25.7544$, and $C = 24.4835$.

3. Contours of three typical detonation waves

The configuration of EFP warhead with a wave shaper is shown in Fig. 2.

As shown in Fig. 2, two propagation paths for the detonation wave are created after the initiator initiates the subsidiary charge, where one path climbs the wave shaper and the other passes through the wave shaper. The detonation wave climbing the wave shaper is called the diffracted detonation wave, and the detonation wave passing through the wave shaper is called the penetrating detonation wave. The times of the diffracted and penetrating detonation waves reaching the liner vary with the change in the thickness of wave shaper. The contours of three typical detonation waves, such as conical detonation wave,

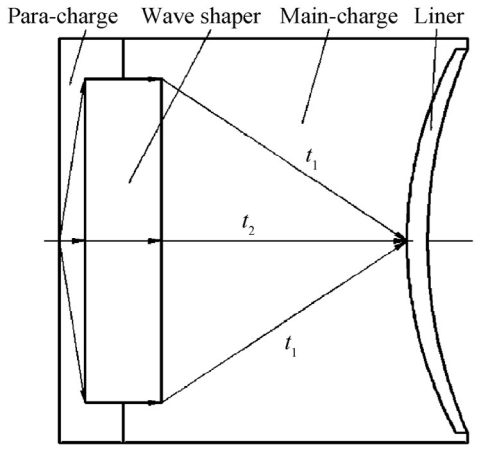

Fig. 2. Configuration of EFP warhead with a wave shaper.

spherical detonation wave, and planar detonation wave (the pseudo planar wave and quasi planar wave all are considered as planar detonation wave), can be created in the main charge.

When the time of diffracted detonation wave reaching the pole t_1 (on the axis) of the liner is less than that of the middle detonation t_2, or if the thickness of wave shaper is larger than the critical thickness, then the diffracted waves collide at the axis of the charge after climbing the wave shaper. If the incident angle is above the critical angle, the Mach wave may emerge at the top of the liner [8,17]. The conical wave emerges in the main charge, as shown in Fig. 3(a). The diffracted detonation wave can greatly increase the length–diameter ratio of EFP [3,18], but the Mach wave may break the nose of EFP [19].

When t_1 is significantly longer than t_2, the diffracted and penetrating detonation waves reach the main charge, but the penetrating detonation wave has a critical function in the main charge. The spherical detonation wave emerges in the main charge, as shown in Fig. 3(b). The spherical detonation wave greatly suppresses the increase in EFP length–diameter ratio [3,18].

When t_1 is approximately equal to t_2, the diffracted and penetrating detonation waves reach the main charge. The diffracted detonation wave cannot collide at the axis of the charge because of the presence of the penetrating detonation wave. Thus, the Mach wave can be avoided. The planar detonation wave may emerge in the main charge, as shown in Fig. 3(c). The diffracted detonation wave can greatly increase the EFP length–diameter ratio, and the nose of EFP is kept integrated because the Mach wave is not present at the top of the liner.

The diameter of the charge is 80 mm and the diameter of the wave shaper is 64 mm. For different thicknesses of the wave shaper, the calculated results of t_1 and t_2 are listed in Table 1.

The shortest path around wave shaper was considered and the turning corner effect was ignored in the present paper. Table 1 shows that, when the thickness of wave shaper increases, t_1 increases minimally, t_2 increases significantly, and t_2 gradually approaches t_1. Therefore, the wave contour in the main charge changes from a spherical detonation wave contour into a planar detonation wave contour with the increase in the

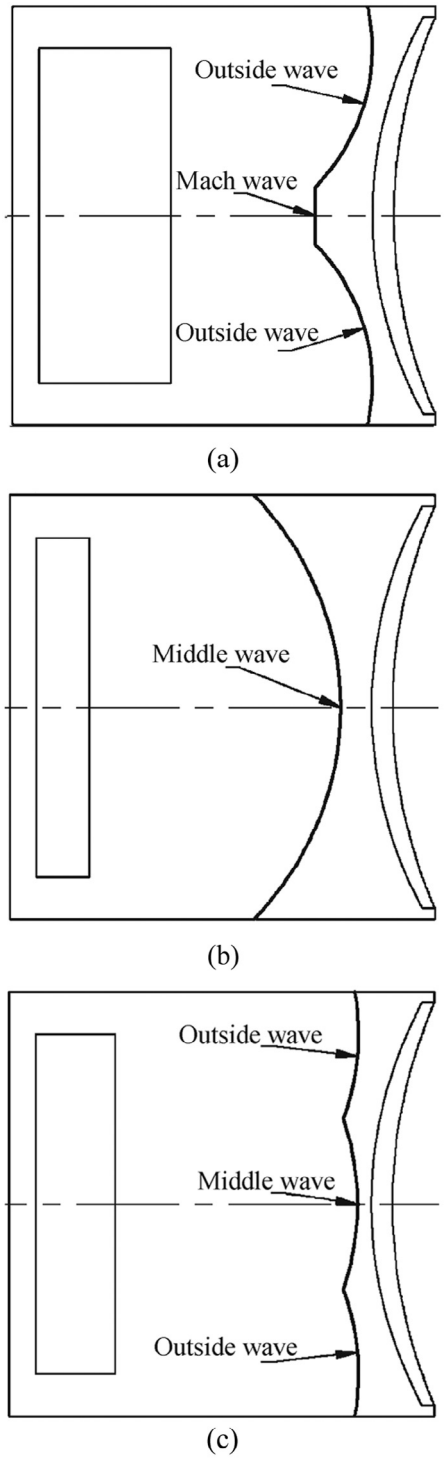

Fig. 3. Contours of three typical detonation waves. (a) Conical detonation wave; (b) Spherical detonation wave; (c) Planar detonation wave.

Table 1
Calculated results of t_1 and t_2 for different thicknesses of wave shaper.

h	5	10	15	20
t_1	13.14	13.23	13.32	13.44
t_2	9.37	9.75	10.34	11.13

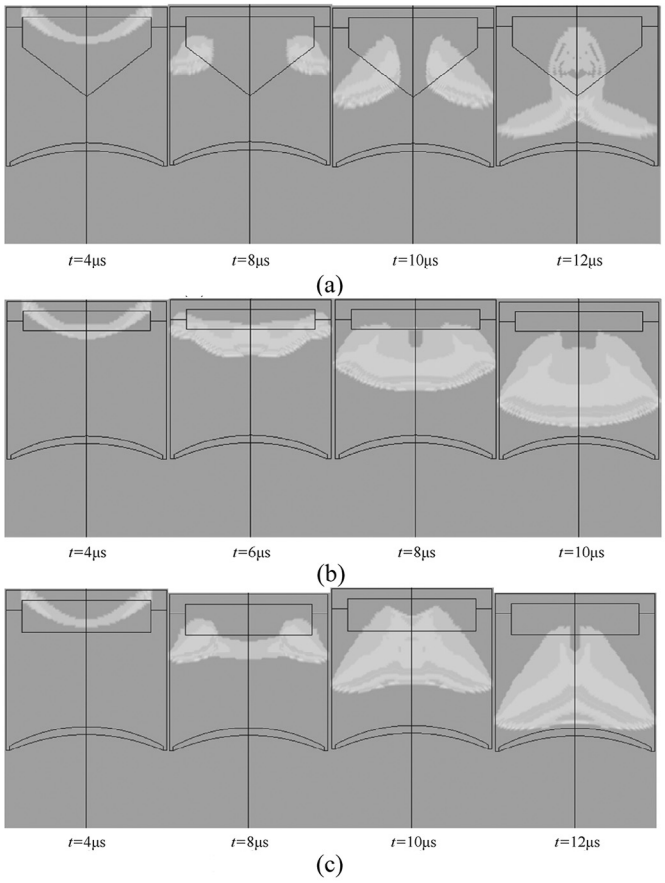

Fig. 4. Simulation results for three typical detonation wave contours. (a) Conical detonation wave; (b) Spherical detonation wave; (c) Planar detonation wave.

thickness of the wave shaper. The area of the penetrating detonation wave decreases, whereas the area of the diffracted detonation wave increases when the thickness of wave shaper is increased. When the thickness of wave shaper is approximately equal to the critical thickness, the area of the penetrating detonation wave is minimal, whereas the area of the diffracted detonation wave maximizes.

4. Simulation research and experimental validation

4.1. Detonation wave contour validation

To verify the reliability of the calculated results, a simulation research was carried out for three warheads by using the LS-DYNA software. The diameters and lengths of all charges are 80 mm, and the diameter of the wave shaper is 64 mm. The thicknesses of the wave shapers are 35 mm, 5 mm, and 16 mm. The 8701 explosive was used in the calculation and the liner was made of copper. The parameters of all material models used in the calculations are found in Refs. [12,20]. The "ignition and growth" model was used as the model of the explosive detonation in the simulation. The detonation wave contours at different times for the three kind of warheads structure are shown in Fig. 4. The shapes of EFP for the three kind of warheads structure are shown in Fig. 5.

As shown in Fig. 4(a), the thickness of the wave shaper is larger than the critical thickness, and the shock wave passing

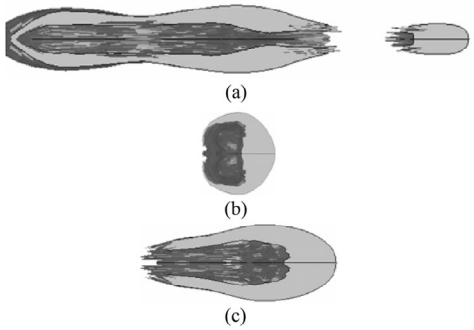

Fig. 5. Shapes of EFP corresponding to the three typical detonation wave contours. (a) Conical detonation wave; (b) Spherical detonation wave; (c) Plane detonation wave.

though the wave shaper cannot initiate the main charge. Thus, no penetrating detonation wave is present in the main charge. The diffracted detonation waves collide at the axis of the charge after climbing the wave shaper, and the Mach wave emerges in the charge. The pressure of the Mach wave is higher than the pressure of detonation wave.

Fig. 4(b) shows that the thickness of the wave shaper is small and the shock wave passing though the wave shaper initiates the main charge. The diffracted and penetrating detonation waves reached the main charge. The penetrating detonation wave has a critical function in the main charge.

As shown in Fig. 4(c), the shock wave passing though the wave shaper initiated the main-charge. The diffracted and penetrating detonation waves reached the main charge and the liner at the same time. However, an overdriven detonation was formed in the charge because the diffracted detonation wave collided with the penetrating detonation wave. However, the pressure of the overdriven detonation wave is slightly higher than the pressure of detonation wave.

The contours of three detonation waves in Fig. 4 are in agreement with those in Fig. 3, thereby indicating that the calculated results in Table 1 are reliable.

As shown in Fig. 5(a), the length–diameter ratio of EFP was large, but the nose of EFP was splitted into two pieces because the diffracted detonation wave greatly increased the length–diameter ratio.

As shown in Fig. 5(b), the length–diameter ratio of EFP is small because the penetrating detonation wave has a critical function in the charge and the spherical wave prevents an increase in the length–diameter ratio of EFP.

As shown in Fig. 5(c), the length–diameter ratio of EFP is large, and the nose of the EFP is completed because the diffracted detonation wave can greatly increase the EFP length–diameter ratio. The nose of EFP was kept intact because no Mach wave was present at the top of the liner.

When the thickness of wave shaper is approximately equal to the critical thickness, the area of the penetrating detonation wave is minimal and the area of the diffracted detonation wave maximizes. The thickness of the wave shaper should be less than and approximately equal to the critical thickness so that the diffracted detonation wave can increase the length–diameter ratio of EFP.

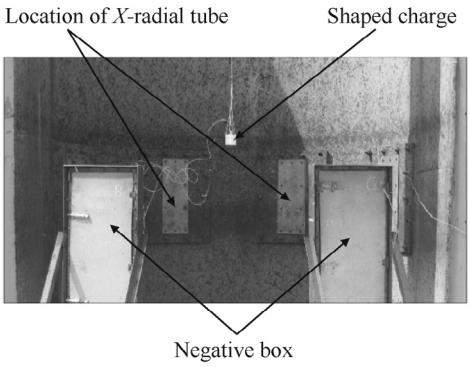

Fig. 6. Layout of X-ray imaging experiment.

Table 2
Comparison between simulated and experimental results.

Item	$V/((m \cdot s^{-1})$	L/mm	d/mm	λ
Simulation	2049	97.4	20.2	4.82
Experiment	1994	107.5	19.2	5.60
Error/%	2.8	9.4	5.2	13.9

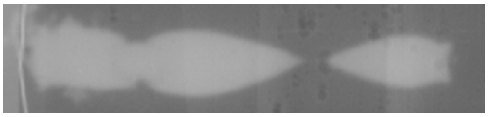

Fig. 7. X-ray image of EFP formation.

4.2. Experimental validation

To verify the reliability of the simulated results, X-ray experiment was carried out on a warhead. The warhead configuration used in the X-ray experiment was the same as the one used in Fig. 5(a). The layout of the X-ray imaging experiment is shown in Fig. 6. The comparison between the simulated and experimental results is shown in Table 2, and the X-ray image of EFP is shown in Fig. 7. The image was taken at 350 μs after the explosive was initiated, at which time the EFP was formed.

In Table 2, v, L, d, and λ represent the velocity, length, diameter, and length–diameter ratio of EFP, respectively.

The results in Table 2 and the image in Fig. 7 indicate that the experimentally generated projectile forms can be successfully reconstructed through simulation, and the simulated results are reliable.

5. Conclusions

1) The contours of three typical detonation waves can be formed in the main charge by changing the thickness of wave shaper. The conical detonation wave can greatly increase the EFP length–diameter ratio, but the Mach wave may break the nose of EFP. The spherical detonation wave suppresses the increase in EFP length–diameter ratio. The planar detonation wave can increase the EFP length–diameter ratio and keep the nose of the EFP intact.
2) The area of the penetrating detonation wave decreases, whereas the area of the diffracted detonation wave increases with the increase in the thickness of wave shaper. The thickness of wave shaper should be less than or approximately equal to the critical thickness so that the planar detonation wave can increase the length–diameter ratio of EFP.

References

[1] Weimann K. Research and development in the area of explosively formed projectiles charge technology. Propellants Explos Pyrotech 1993;18(5):294–8.
[2] Moser R, Fong R, Ng W. Increasing explosively formed penetrator (EFP) warhead performance with more powerful explosives (MPE). In: Proc. 20th international symposium on ballistics, September 23–27, Orlando, Florida, USA; 2002. p. 573–6.
[3] Blache A, Weimann K. Generation of different detonation wave contours. In: Proc. 18th international symposium on ballistics, September 23–28, San Francisco, CA, USA; 1996. p. 337–46.
[4] Weimann K. Performance of tantalum, copper, and iron EFPs against steel targets. In: Proc. 15th international symposium on ballistics, May 21–24, Jerusalem, Israel; 1995. p. 399–404.
[5] Zhang XF, Qiao L. Studies on jet formation and penetration for a double-layer shaped charge. Combust Explos Shock Waves 2011;47(2):241–8.
[6] Murphy M, Weimann K, Doeringsfeld K, Speck, J. The effect of explosive detonation wave shaping on EFP shape and performance. In: Proc. 13th international symposium on ballistics, June 1–3, Stockholm, Sweden; 1992. p. 449–56.
[7] Steinmann F, Lösch C. Multimode warhead technology studies. In: Proc. 21th international symposium on ballistics, April 19–23, Adelaide, Australia; 2004. p. 728–35.
[8] Zhang YG, Zhang XF, He Y, , Qiao L Detonation wave propagation in shaped charges with large wave-shaper. In: Proc. 27th international symposium on ballistics, April 22–26, Freiburg, Germany: 2013. p. 770–82.
[9] Men JB, Jiang JW, Luo J. Numerical simulation research on the influence of sensing elements on EFP forming. J Ballist 2005;17(1):67–71 [in Chinese].
[10] Zhang XF, Chen HW, Zhao YS. Study on shaped charge technique of small diameter which have high velocity EFP. J Project Rock Miss Guid 2003;23(3):107–9 [in Chinese].
[11] Chen L, Wu JY, Fang Q, Ke JS, Feng CG. Investigation of solid explosives initiation on under shock waves. Chin J Explos Propellants 2004;27(1):1–4 [in Chinese].
[12] Li WB, Wang XM, Li WB. The effect of annular multi-point initiation on the formation and penetration of an explosively formed penetrator. Int J Impact Eng 2010;37(4):414–24.
[13] Wang HF, Feng SS. An approximate theoretical model for the attenuation of shock pressure in solid materials. Acta Armamentarn 1996;17(1):79–81 [in Chinese].
[14] Beijing Institute of Technology. Explosion and action. Beijing: Defence Industry Press; 1979.
[15] Wang ZS, Liu YC, Zhen M, Zhang J. Study on the attenuating model of detonation shock wave in the PMMA gap. J Basic Sci Eng 2001;9(4):316–19 [in Chinese].
[16] Wu YH. Study on the shock initiation phenomenon for heterogeneous condensed explosives [Ph.D. thesis], Changsha: Hunan University, 2006 [in Chinese].
[17] Dunne B. Mach reflection of detonation waves in condensed high explosives. Phys Fluids 1964;7(10):1707–12.
[18] Gazeaud G. Explosively formed projectile: optimization. In: Proc. 13th international symposium on ballistics, June 1–3, Stockholm, Sweden; 1992. p. 473–9.
[19] Zhu CS, Huang ZX, Zu XD, Xiao QQ. Mach wave control in explosively formed projectile warhead. Propellants Explos Pyrotech 2014;39(6):909–15.
[20] Murphy MJ, Lee EL, Weston AM, Williams AE. Modeling shock initiation in Composition B.Williams AE Proc. 10th international detonation symposium, July 12–16, Boston, Massachusetts; 1993. p. 963–70.